ANTICANCER RESEARCH *40*: 2675-2685 (2020)
doi:10.21873/anticanres.14238

Inhibition of Jurkat T Cell Growth by *N*-farnesyl-norcantharimide Through Up-regulation of Tumor Suppressor Genes and Down-regulation of Genes for Steroid Biosynthesis, Metabolic Pathways and Fatty Acid Metabolism

JIN-YI WU[1*], EN-TUNG TSAI[2*], FANG-YU YANG[1], JUI-FENG LIN[3,4], HUI-FEN LIAO[5], YU-JEN CHEN[6] and CHENG-DENG KUO[2,7,8]

[1]*Department of Microbiology, Immunology and Biopharmaceutics, College of Life Sciences, National Chiayi University, Chiayi, Taiwan, R.O.C.;*
[2]*Department of Medical Research, Taipei Veterans General Hospital, Taipei, Taiwan, R.O.C.;*
[3]*Division of Neurosurgery, Department of Surgery, Mackay Memorial Hospital, Taipei, Taiwan, R.O.C.;*
[4]*Institute of Traditional Medicine, National Yang-Ming University School of Medicine, Taipei, Taiwan, R.O.C.;*
[5]*Department of Biochemical Science and Technology, National Chiayi University, Chiayi, Taiwan, R.O.C.;*
[6]*Department of Radiation Oncology, Mackay Memorial Hospital, Taipei, Taiwan, R.O.C.;*
[7]*Division of Chest Medicine, Department of Internal Medicine, Changhua Christian Hospital, Changhua, Taiwan, R.O.C.;*
[8]*Tanyu Research Laboratory, Taipei, Taiwan, R.O.C.*

Abstract. *Background/Aim: To evaluate the anti-cancer mechanism of N-Farnesyl-norcantharimide (NC15). Materials and Methods: The viability of NC15-treated human leukemic Jurkat T (JKT) cells was assessed using the Kit-8 cell counting method. Flow cytometry analysis, human apoptosis antibody array assay, and whole genome sequencing were adopted to investigate the mechanism underlying the anti-cancer activity of NC15 in JKT cells. Results: The growth inhibition rates of NC15 in JKT cells were about 80% and 95% after treatment with 8 μmol/l NC15 for 24 and 48 h, respectively. The percentages of NC15-treated JKT cells in the sub-G_1 phase at 24 and 48 h were 22.0% and 34.3%, respectively, in contrast to the 1.5% in the control. Next-generation sequencing showed that many tumor suppressor genes (TSG) were up-regulated, while many genes associated with steroid biosynthesis, metabolic pathways, and fatty acid metabolism were down-regulated. Conclusion: NC15 can reduce the cell viability and increase the percentage of JKT cells in the sub-G_1 phase by up-regulating TSG and related genes, and down-regulating the genes for steroid biosynthesis, metabolic pathways and fatty acid metabolism, instead of through apoptosis.*

Acute T lymphoblastic leukemia (T-ALL) is one of the most common childhood cancers with very poor prognosis (1). A quarter of childhood T-ALL patients have relapsed within 5 years of treatment with very poor prognosis (2). The survival rate of patients with T-ALL within 5 years is less than 25% (3). Therefore, it is necessary to search for more efficient yet less toxic anti-cancer drugs for leukemia.

The Jurkat T (JKT) cell line established from the peripheral blood of a 14 years old boy with T-ALL in the late 1970s was used in this study (4). Phorbol 12-myristate 13-acetate plus ionomycin (PMA + ION) are often used in the study of the underlying mechanism of anti-cancer drugs because PMA + ION can activate JKT cells to produce high levels of interleukin-2 (IL-2) (5-8), and activate the JKT cells *via* a PKC-Ras signaling pathway (7, 8).

Mylabris, a species of blister beetle (*Mylabris phalerata* Pall.), has been used in the treatment of many kinds of malignancies in traditional oriental medicine for two thousand years (9-12). Mylabris-derived Cantharidin is a potent serine/threonine protein phosphatase 1 (PP1) and protein phosphatase 2A (PP2A) inhibitor (13-15). Though Cantharidin has anti-cancer properties (16, 17), its clinical applications are limited because of its toxicity towards the kidneys and the urinary system (18, 19).

*These Authors contributed equally to the present study.

Correspondence to: Cheng-Deng Kuo, Department of Medical Research, Taipei Veterans General Hospital, Taipei 112, Taiwan, R.O.C. Tel: +886 932981776, e-mail: cdkuo23@gmail.com

Key Words: N-farnesyl-norcantharimide, Jurkat T cells, next-generation sequencing, tumor suppressor gene, biosynthesis.

Norcantharidin (NCTD) derived from demethylation of Cantharidin has been shown to be effective towards many kinds of cancers including hepatocellular cancer (20), gallbladder malignancy (21), leukemia (22), and colorectal cancer (23). NCTD is able to prolong the survival of nude mice transplanted with human HepG2 cells by inhibiting the growth of tumor cells (24). The NCTD has an anti-cancer activity similar to that of Cantharidin (25, 26) with a lower cytotoxicity toward normal cells as compared to Cantharidin (26-28), and has less nephrotoxicity and other side effects than Cantharidin in clinical practice (9).

N-Farnesyl-norcantharimide ($C_{23}H_{33}NO_3$, denoted as NC15), is a newly synthesized NCTD derivative (29). Figure 1 shows the chemical structures of NCTD and NC15. NC15 has high anti-cancer activity in cell models, and can induce G_2/M arrest and induce cell apoptosis on mouse leukemic L1210 cells (30). NC15 has been found to prolong the survival of mice and reduce the weight of the tumor mass in a mouse leukemia model (30). This study investigated the mechanism underlying the anti-cancer activity of NC15 in JKT cells.

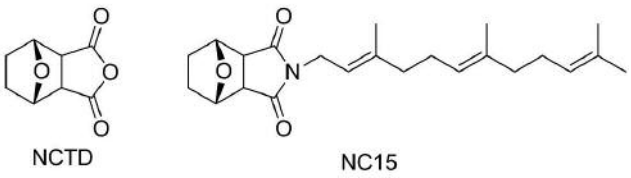

Figure 1. *The chemical structures of NCTD and NC15.*

Materials and Methods

Chemical reagents. Both NCTD and NC15 (Figure 1) were synthesized and characterized in the previous report (29). Anti-Caspase-9, Caspase-8, Caspase-3, Bcl-2, BAX, Cytochrome C and Actin antibodies were purchased from the Cell Signaling Technology (Danvers, MA, USA). The anti-PARP antibodies were purchased from the Thermo Fisher Scientific (Waltham, MA, USA).

Cytotoxicity assay. The IC_{50} values of the cytotoxic effects of NC15 on JKT cells were calculated using the dose–response curve. The JKT cells [Clone E6-1, Bioresource Collection and Research Center (BCRC) number: 60424] and human normal lymphoblast (HNL, BCRC number: 08C0058) were cultured in RPMI 1640 medium (Biological Industries, Kibbutz Beit Haemek, Israel) plus 10% heat-treated fetal bovine serum (FBS) (Hyclone, Logan, UT, USA) in a humidified 5% CO_2 incubator at 37˚C. Both JKT and HNL cells were plated in 96-well plates at a density of 1×10^4 cells/well. The cells were treated with 0, 2, 4, 6, and 8 μmol/l NC15 for 24 and 48 h. After incubation, the viability of JKT and HNL cells was assessed by using CCK-8 (Sigma, St Louis, MO, USA). The detection wavelength was set at 450 nm.

Total proteins isolation. The untreated and NC15-treated JKT cells were harvested by centrifugation at 200 × *g* for 10 min at 4˚C. The cell pellets were washed once by ice-cold phosphate-buffered saline, re-suspended in 100 μl lysis buffer [10X RIPA buffer, 200 mM sodium orthovanadate (Na_2VO_3), 7X protease inhibitor, and 10X phosphatase inhibitor], and then placed on ice for 30 min. The cells in the suspension were ruptured by vortexing and centrifuged at 13000×g for 10 min at 4˚C. The supernatants of ruptured cells were collected for later analyses.

Flow cytometry analysis. Apoptosis array assay was performed using flow cytometry analysis to study whether or not the apoptosis is the main anti-cancer mechanism of NC15. JKT cells plated in 6-well plates at a density of 1×10^6 cells/well were treated with NC15 at the IC_{50} concentration for 24 and 48 h. To determine the populations of apoptotic and necrotic cells (sub-G_1 and G_0 cell fraction), the JKT cells were harvested, fixed with cold 70% ethanol, stored at –20˚C overnight, and treated with with 0.2% Triton X-100, 0.1 mg/ml RNase A (Sigma, MO, USA) and stained with 20 μmol/l Propidium iodide (PI) at 37˚C in the dark for 30 min. The NC15-treated cells were stained with Annexin V-FITC (eBioscience, San Diego, CA, USA) in Annexin V staining buffer at 25˚C for 10 min, and counterstained with 20 mg/ml PI in binding buffer solution without phenol red, and then analyzed by a FACS flow cytometer (BD Biosciences, Franklin Lakes, NJ, USA) to evaluate the JKT cells in the early stages of apoptosis.

Human apoptosis antibody array. To examine whether or not apoptosis is the main anti-cancer mechanism of NC15, human apoptosis antibody array assay was performed on JKT cells treated with or without NC15 for 1 day. After that, the protein extracts of JKT cells were harvested and 200 μg of each protein extract were analyzed by using the human apoptosis antibody array kit (RayBiotech, Norcross, GA, USA). To capture the chemiluminescence signals, the membranes were exposed to the autoradiography film for various periods of time. The AlphaImager HP System (ProteinSimple, San Jose, CA, USA) was employed to quantify the images with chemiluminescence signals within the linear ranges. The chemiluminescence signals of the negative control spots on each membrane were averaged and then subtracted from that of each experimental spot. If the value of the chemiluminescence signal exceeded both the averaged local background and the averaged valid negative control values, the signal was considered valid (31). The valid chemiluminescent signal was normalized by the values of the positive control spots. The fold changes in the chemiluminescence signals of each spot were divided by the value of the valid signals at the corresponding spot on the minus NC15 membrane. Finally, the averaged fold changes and the standard deviations of each protein were calculated.

Next-generation sequencing. Whole genome sequencing of NC15-treated JKT cells was performed using next-generation sequencing (NGS) (32-36) to determine which genes in the JKT cells were regulated by NC15 treatment.

RNA quantification and qualification. Both RNA degradation and contamination were monitored on 1% agarose gels. The purity of the RNA was assessed using NanoPhotometer® spectrophotometer (IMPLEN, Westlake Village, CA, USA) (37). The concentration of RNA was determined using Qubit® RNA Assay Kit and Qubit® 2.0 Flurometer (Life Technologies, Carlsbad, CA, USA). The

integrity of the RNA was assessed using RNA Nano 6000 Assay Kit and the Bioanalyzer 2100 system (Agilent Technologies, Santa Clara, CA, USA).

Library preparation for transcriptome sequencing. Three μg of RNA per sample were used as the input material for the preparation of RNA sample. Sequencing libraries were generated using NEBNext® Ultra™ RNA Library Prep Kit for Illumina® (New England Biolabs (NEB), San Diego, CA, USA). The index codes were added to the attribute sequences to each sample. In short, the mRNA was purified from the total RNA using poly-T oligo-attached magnetic beads. The fragmentation was then carried out in the NEBNext first strand synthesis reaction buffer (5X) using divalent cations at 72˚C. Random hexamer primer and M-MuLV reverse transcriptase (RNase H–) was used to synthesize the first strand cDNA. After that, the second strand cDNA was synthesized using DNA Polymerase I and RNase H. Through the help of exonuclease/polymerase activities, the remaining overhangs were converted into blunt ends. After the completion of adenylation at the 3' ends of the DNA fragments, the NEBNext Adaptor with hairpin loop structure was ligated and then used for hybridization. In order to select appropriate cDNA fragments of about 150~200 bp, the library fragments were purified with the help of the AMPure XP system (Beckman Coulter, Beverly, MA, USA). Before PCR, 3 μl of USER enzyme (NEB) were used with the size-selected, adaptor-ligated cDNA at 37˚C for 15 min, followed by incubation at 95˚C for 5 min. The PCR was performed using the Phusion® High-Fidelity DNA polymerase (NEB), universal PCR primers, and Index (X) primer. The PCR products thus obtained were purified using the AMPure XP system. At last, the library quality of the products was assessed by the Agilent Bioanalyzer 2100 system (38).

Clustering and sequencing. By using the TruSeq PE Cluster Kit v3-cBot-HS (Illumina, San Diego, CA, USA), the clustering of the index-coded samples was performed on a cBot Cluster Generation System following the manufacturer's instructions. The library preparations were sequenced on the Illumina HiSeq 2500 PE150 platform (Illumina) after cluster generation. The 125 bp/150 bp paired-end reads were then generated (38).

Quality control. Through in-house perl scripts, the raw data or raw reads of fastq format were processed. At this step, the clean data or clean reads were obtained when the reads containing adapter, the reads containing ploy-N, and the low quality reads from the raw data were removed. Meanwhile, the Q20, Q30 and GC containing the high quality clean data were calculated to perform all downstream analyses (39).

Reads mapping to reference genome. The gene model annotation files and reference genome were downloaded directly from the genome website. Bowtie v2.2.3 was used to build the index of the reference genome, and TopHat v2.0.12 was used to align the paired-end clean reads to the reference genome. Since the TopHat can generate a database of splice junctions based on the gene model annotation file and yield a better mapping result compared with other non-splice mapping tools (39), it was selected and used as the mapping tool.

Quantification of gene expression and differential expression analysis. The reads numbers mapped to each gene were counted using the HTSeq v0.6.1. Based on the length of the gene and reads count mapped to this gene, the fragments per kilobase of transcript per million mapped reads (FPKM) of each gene were calculated (40). For the estimation of gene expression levels, the FPKM is currently the most commonly used method because it takes into account the effects of both sequencing depth and gene length on the reads count simultaneously. The read counts of each sequenced library were adjusted using the edgeR program package through one scaling normalized factor before differential gene expression analysis. The DEGSeq R package (1.20.0) was employed to analyze the differential expression. The Benjamini & Hochberg method was used to adjust the *p*-values. A corrected *p*-value of 0.005 and a $\log_2$ (fold change) of 1 were adopted as the threshold of significantly different expression (41).

GO and Kegg enrichment analysis. To correct the bias caused by gene length, the GOseq R package was used to perform the Gene Ontology (GO) enrichment analysis of the differentially expressed genes. GO terms whose corrected *p*-Values were smaller than 0.05 were regarded as significantly enriched by differentially expressed genes. The Kyoto Encyclopedia of Genes and Genomes (KEGG) database was a resource constructed from molecular-level information for the understanding of high-level functions and utilities of the biological system, comprizing of the cell, organism and ecosystem (42). The KOBAS webserver software was employed to test the statistical enrichment of differentially expressed genes in the KEGG pathways (43, 44).

PPI analysis of differentially expressed genes. The protein-protein interactions (PPI) analysis of differentially expressed genes was performed using the STRING database. For the species in the database, the networks were constructed by extracting the target gene list in the STRING database in accordance with the known interactions of selected reference species (45). Otherwise, the search protein database Blastx v2.2.28 was utilized to align the target gene sequences with the selected reference protein sequences. .

Statistical analysis. The experimental data of this study were expressed as means±standard deviation (SD) when appropriate. Student's *t*-test was employed to compare the study data with the control values. A $p<0.05$ was considered to indicate statistically significant differences compared to the control values. All statistical analyses were performed using the GraphPad Prism software (GraphPad Software Inc., La Jolla, CA, USA).

Results

NC15 inhibited the growth of JKT cells. To determine the inhibitory effects of NC15 on the growth of JKT and HNL cells, their viability was assessed using Kit-8 cell counting method after treatment with 0, 2, 4, 6 or 8 μmol/l NC15 for 24 and 48 h. Figure 2a and b show that the growth of JKT cells was inhibited by NC15 in a dose- and time-dependent manner. The IC_{50} of NC15 inhibition on the growth of JKT cells at 24 and 48 h was found to be 2.51 and 2.54 μmol/l, respectively. When 8 μmol/l of NC15 was added to the JKT cells for 24 and 48 h, the inhibition rate of NC15 on JKT cells was increased to about 40%, as compared to the cells without NC15 treatment. Figure 2a and b also show that

there were no significant differences in the growth of HNL cells treated with 0, 2, or 4 μmol/l NC15. Thus, the NC15 could inhibit the growth of JKT cells, but has mild inhibitory effects on the growth of HNL cells.

Cell cycle analysis. To determine whether apoptosis is the main mechanism underlying the growth inhibitory effects of NC15, JKT cells were treated with the IC_{50} concentrations of NC15 (2.51 and 2.54 μmol/l) for 24 and 48 h, and then the number of cells in the sub-G_1 phase was assayed using flow cytometry with PI staining. Figure 3a show that only a small number of apoptotic cells was found in untreated cells. Figure 3 further shows that, compared to the untreated cells, the percentages of NC15-treated cells in the sub-G_1 phase at 24 and 48 h were significantly increased, while the percentages of NC15-treated cells in the G_1 phase at 24 h and 48 h were significantly decreased. However, the percentages of NC15-treated cells in both the S and G_2/M phases were not significantly different from the untreated cells. Thus, NC15 could inhibit the growth of JKT cells through interference with their cell cycle.

Effect of NC15 on cell death. To assess the possibility of NC15-induced apoptosis in JKT cells, the number of apoptotic cells after NC15 treatment was determined using flow cytometry plus Annexin V/PI staining. Flow cytometry analysis demonstrated that the number of Annexin V-positive/PI-negative cells (early apoptosis) and Annexin V-positive/PI-positive cells (trace amount of late apoptosis) was slightly increased in parallel with the concentration of NC15. Figure 4 shows that the early/possibly late apoptosis ratios were 0.8/2.8, 1.2/1.7, 1.9/2.3, 1.8/3.6, 2.1/7.4 in the untreated cells versus the cells treated with 2, 4, 6, and 8 μmol/l NC15, respectively. The result of Annexin-V/PI analysis suggested that NC15 may induce trace amount of late apoptosis, but not early apoptosis, in JKT cells. Whether or not late apotosis is the mechanism of cytotoxicity of NC15 over JKT cells was investigated in the following apoptosis array analysis.

NC15 did not alter the levels of apoptosis-related proteins. To assess whether apoptosis is the main mechanism of cell death, the JKT cells were treated with NC15 (0, 2, 6, and 8 μmol/l) for 24 h, and then lysed. The apoptotic markers were screened using apoptosis array. Figure 5 shows that there were no significant differences between the treated and untreated cells regarding bad, bax, BID, bcl-2, Caspase-3, Caspase-8, Cytochrome C, Fas, Fas ligand, and HSP70. This result suggested that NC15 did not induce apoptosis in JKT cells.

NC15 affected metabolic and biosynthetic pathways in JKT cells. To understand the underlying mechanism of cell death

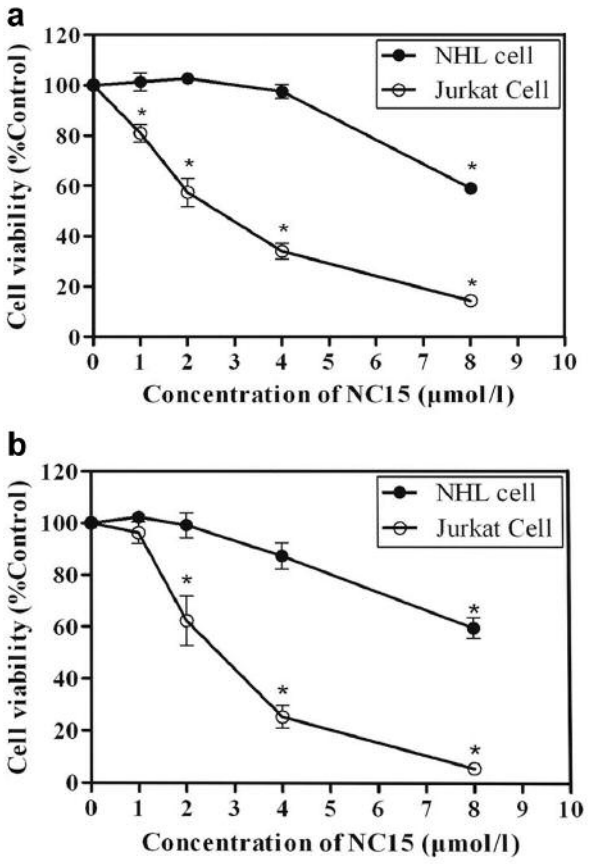

Figure 2. *N-Farnesyl-norcantharimide (NC15) inhibited the growth of human leukemic Jurkat T (JKT) cells and human normal lymphoblast (HNL) cells. The cells were plated at the beginning concentration of 1×10^4 cells/ml, treated with 0, 1, 2, 4, and 8 μmol/l of NC15 for 24 or 48 h. The total cell number of the control and NC15 treated groups were counted and plotted. The results are expressed as means±SD for three independent experiments performed in triplicate. (a) 24 h; (b) 48 h. *p<0.05 was considered significantly different from the JKT cells. NC15, N-farnesyl-norcantharimide.*

in the NC15-treated JKT cells, the cDNA of the JKT cells exposed to NC15 for 24 h was amplified using RT-PCR, and whole genome sequencing was performed using next-generation sequencing (NGS, Illumina). The data suggested that the tumor suppressor genes (TSG) including cytochrome B-245 alpha chain (CYBA) for NADPH, cyclin-dependent kinase inhibitor 1B (CDKN1B) for P27, activating transcription factor 4 (ATF4) for CREB3, and the genes for serine metabolism and aminoacyl-tRNA biosynthesis were up-regulated, while the genes for steroid biosynthesis, metabolic pathways, and fatty acid metabolism were down-regulated (Tables I and II). This result suggested that NC15 might inhibit the viability and proliferation of JKT cells through the up-regulation of the above-mentioned TSG and the genes for serine metabolism and aminoacyl-tRNA

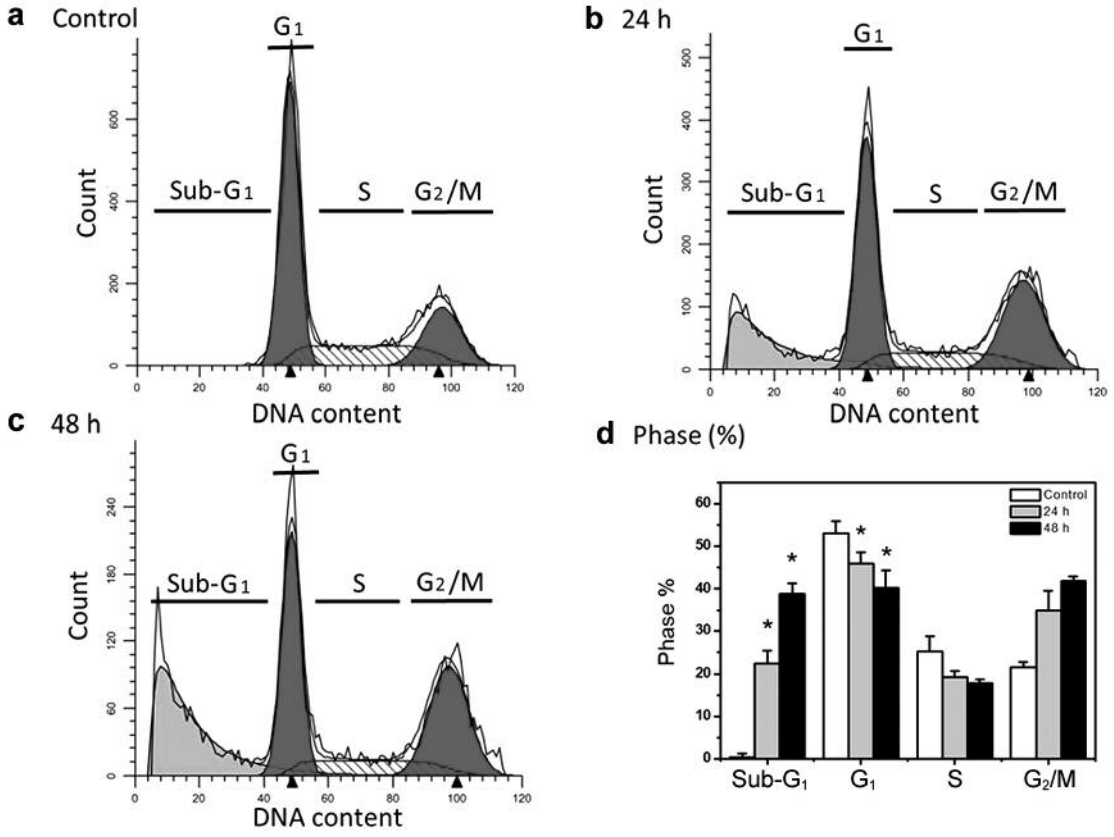

Figure 3. *The sub-G1 DNA content in JKT cells was assayed by flow cytometry. Jurkat T cells were treated with and without 2.51 and 2.54 μmol/l NC15 for 24 and 48 h, respectively. After fixing in 70% ethanol, the cells were stained with Propidium iodide (PI) and assayed by flow cytometry. (a) Untreated control; (b) 24 h; (c) 48 h; (d) percent of cells in cell cycle sub-G_1 phase (%). The percentages of cells undergoing apoptosis observed at 24 h and 48 h are representatives of three independent experiments, where similar results were obtained. *p<0.05 was considered significantly different from the control cells.*

biosynthesis, and the down-regulation of the genes responsible for steroid biosynthesis, metabolic pathways, and fatty acid metabolism.

Discussion

NC15 is a newly synthesized NCTD derivative with better anti-cancer activity than NCTD towards cell viability and proliferation in JKT cells. It has been shown that NC15 had higher cytotoxicity and anti-proliferative effects on human liver carcinoma HepG2 cell line, yet had lower cytotoxic effect on normal murine embryonic liver BNL CL.2 cells (29). In this study, NC15 was shown to decrease the viability of cells, increase the percentage of cells in the sub-G_1 phase and induce trace amount of late apoptosis in JKT cells. Though the mechanism of cytotoxic effects of NC15 on JKT cells is not clear yet, apoptosis might not be the main mechanism of anti-cancer effects of NC15 on JKT cells, because there were no significant differences between treated and untreated JKT cells in the expressions of bad, bax, BID, bcl-2, Caspase-3, Caspase-8, Cytochrome C, Fas, Fas ligand, and HSP70 (Figure 5), and the progression of JKT cells could be inhibited by NC15 through its effects on the expression of TSG and genes for serine metabolism, aminoacyl-tRNA biosynthesis, steroid biosynthesis, metabolic pathways, and fatty acid metabolism in JKT cells (Table I and II).

High-throughput sequencing or next-generation sequencing (NGS) technology has dramatically improved our capability to characterize various kinds of cancers at the genomic level by cataloguing all mutations, aberrations in copy number and somatic rearrangements in the entire cancer genome (46, 47). NGS has significantly accelerated biological and biomedical research by facilitating inexpensive, routine, widespread, and comprehensive analyses of genomes, transcriptomes and interactomes, without requiring significant production-scale efforts (48). In the present study, gene expression of the JKT cells was analyzed using NGS technologies. The changes in gene expression of JKT cells represented the effects of

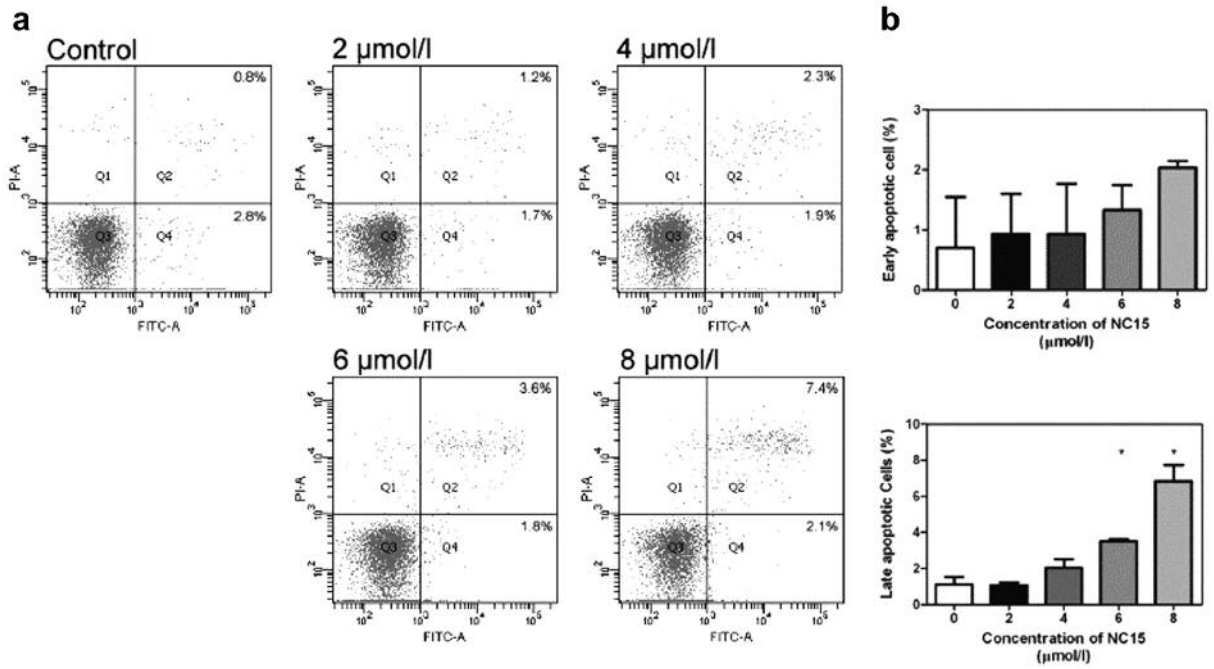

Figure 4. *Examination of apoptosis in JKT cells treated with different concentrations of NC15 by Annexin V/PI staining. JKT cells were treated with 0, 2, 4, 6, and 8 μmol/l NC15 for further 24 h. The cells were stained with Annexin V/PI and assayed by flow cytometry. (a) Apoptosis in JKT cells was assessed by Annexin V/PI double staining; (b) Apoptosis rate of early and trace amount of late apoptotic cells. *p<0.05 was considered significantly different from the control cells.*

NC15 treatment on the JKT cells. We speculate that altered protein levels in NC15-treated JKT cells due to up- and down-regulation of genes may result in the disturbance of many metabolic pathways of the JKT cells, leading to cell death. This might be the underlying mechanism of cell death in the JKT cells after treatment with NC15, instead of apoptosis.

The NGS data showed that the over-expressed TSG after treatment with NC15 in JKT cells included the CYBA (NADPH), CDKN1B (P27), and ATF4 (CREB3) genes that control the progression of cell cycle. The mechanisms controlling cell cycle progression are frequently lost in human cancer cells. The cell cycle is driven forward by cyclin-dependent kinases (CDK), and the inhibitors of CDK (CDKI) are important regulators of CDK. Thus, CDKIs negatively regulate cell cycle progression, and are responsible for cell cycle arrest at the G_1 phase (49-52). The down-regulation of CDKI or TSG can lead to increased cell proliferation. Since NC15 could inhibit the viability of JKT cells by increasing the percentage of cells in the sub-G_1 phase and G_0-G_1 arrest, CDKI might be involved in cell cycle arrest at the G_1 phase in JKT cells.

Recently, the links between metabolic enzymes and oncogene-induced signal transduction have attracted increasing interest because the metabolic pathways are targets of cancer chemotherapy. The assessment of the metabolic pathways and their interplay in cancer cells should be important for the understanding of the transformation mechanisms, the mechanisms of neo-growth and cancer cell drug resistance, and for the identification of potential drugs specific for cancer cells (53, 54). In this study, we found that the expression of TSG and the genes responsible for serine metabolism and aminoacyl-tRNA biosynthesis was up-regulated (Table I), while the expression of the genes responsible for steroid biosynthesis, metabolic and fatty acid metabolism enzymes in JKT cells was down-regulated (Table II) following treatment with NC15. These changes in gene expressions might lead to instability and even breakdown of the metabolic functions of the cells and the disturbance of cell cycle, leading to cell death. This might be the main mechanism of the anti-cancer activity of NC15 on JKT cells. The destruction of cancer cells through the derangement of their metabolic pathways might be termed "metabolic killing". Thus, the derangement and disturbance of metabolic pathways in cancer cells might be a target for developing potential anti-cancer drugs.

The accumulation of cells in the sub-G_1 phase of the cell cycle may not be evidence of apoptosis, because the observed DNA fragmentation may also be caused by necrosis or necroptosis. Annexin-V/PI analysis indicated that NC15 may induce trace amount of late apoptosis in JKT cells (Figure 4), but an apoptosis array analysis showed that there

(a) Control

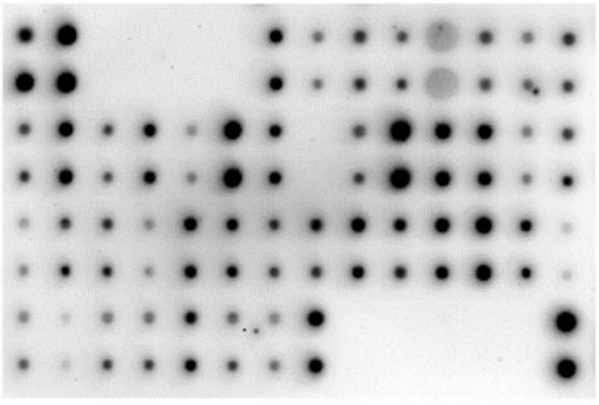

(b) NC15 2 μmol/l

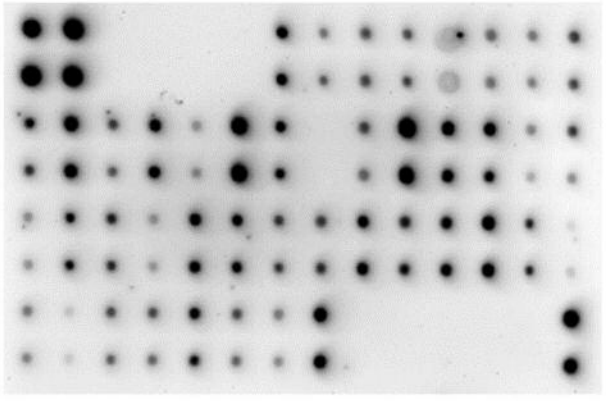

(c) NC15 6 μmol/l

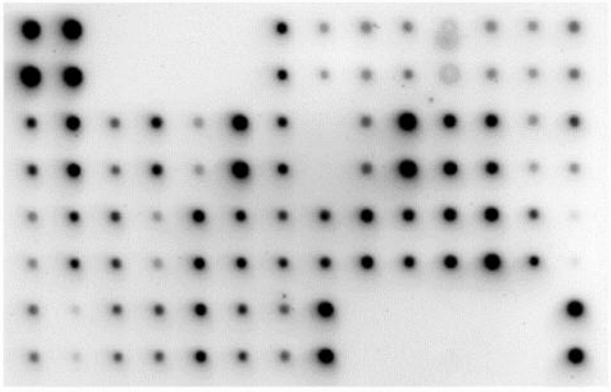

(d) NC15 8 μmol/l

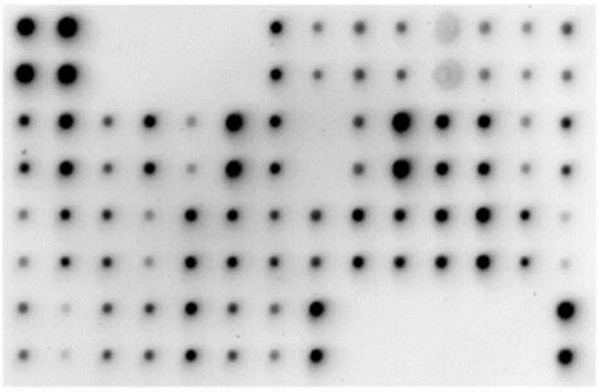

(e) Human apoptosis maps

Each antibody is spotted in duplicate vertically	A	B	C	D	E	F	G	H	I	J	K	L	M	N
1	POS	POS	NEG	NEG	BLANK	BLANK	bad	bax	bcl-2	bd-w	BID	BIM	Caspase-3	Caspase-8
2														
3	CD40 (TNFRSF5)	CD40 Ligand (TNFSF5)	dAP-2	CytoC	DR6 (TNFRSF21)	Fas (Apo-1)	Fas Ligand (TNFSF6)	BLANK	HSP27	HSP60	HSP70	HTRA2	IGF-1	IGF-2
4														
5	IGFBP-1	IGFBP-2	IGFBP-3	IGFBP-4	IGFBP-5	IGFBP-6	IGF-1R	Livin	P21	P27	P53	SMAC	Survivin	TNF R1 (TNFRSF1A)
6														
7	TNFR II (TNFRSF1B)	TNF alpha	TNF beta	TRAIL R1 (TNFRSF10A)	TRAIL R2 (TNFRSF10B)	TRAIL R3 (TNFRSF10C)	TRAIL R4 (TNFRSF10D)	XIAP	BLANK	BLANK	NEG	NEG	NEG	POS
8														

Figure 5. *Examination of apoptosis in JKT cells treated with different concentrations of NC15 by human apoptosis array. JKT cells were treated with 0, 2, 6, and 8 μmol/l NC15 for 24 h. The cell lysates were collected and 200 μg of each were analyzed by human apoptosis array. (a) Untreated; (b) 2 μmol/l; (c) 6 μmol/l; (d) 8 μmol/l; (e) array maps.*

was no up-regulation of proteins associated with apoptosis (Figure 5). Thus, necrosis or necroptosis might not be the mechanism underlying the accumulation of NC15-treated JKT cells in the sub-G_1 phase.

Cell apoptosis can be divided into early and late apoptosis. When apoptosis is measured over time, the cells can undergo transformation from Annexin V negative/PI negative (no apoptosis) to Annexin V positive/PI negative (early apoptosis

Table I. *Up-regulated genes in NC15-treated JKT cells as compared with the control cells.*

Associated gene	Log2 fold change	*p*-Value
Tumor suppressor gene (TSG)		
CYBA	0.92036	9.97×10^{-15}
CDKN1B	0.53978	3.26×10^{-6}
ATF4	0.36309	9.22×10^{-5}
Serine metabolism		
CBS	0.91916	1.15×10^{-6}
PHGDH	0.76164	5.29×10^{-15}
PSAT1	0.68002	1.74×10^{-12}
PSPH	0.49351	4.92×10^{-5}
Aminoacyl-tRNA biosynthesis		
MARS	0.57117	3.61×10^{-9}
CARS	0.48889	4.71×10^{-6}
SARS	0.42555	1.91×10^{-5}
LARS	0.37107	1.80×10^{-4}

Whole gene expression analysis on NC15-treated JKT cells by Next Generation Sequencing. Data are expressed as the *p*-values which have been adjusted using the Benjamini & Hochberg method. Corrected *p*-value of 0.005 was set as the threshold for significantly differential expression. CYBA: Cytochrome B-245 Alpha Chain; CDKN1B: Cyclin dependent kinase inhibitor 1B; ATF4: activating transcription factor 4; CBS: cystathionine beta synthase; PHGDH: phosphoglycerate dehydrogenase; PSAT1: phosphoserine aminotransferase 1; PSPH: phosphoserine phosphatase; MARS: methionyl-trna synthetase; CARS: cysteinyl-TRNA synthetase; SARS: seryl-TRNA synthetase; LARS: leucyl-TRNA synthetase.

Table II. *Down-regulated genes in NC15-treated JKT cells as compared with the control cells.*

Associated gene	Log2 fold change	*p*-Value
Steroid biosynthesis		
TM7SF2	–0.88097	1.04×10^{-5}
MSMO1	–0.84438	6.26×10^{-8}
HSD17B7	–0.71839	1.90×10^{-5}
NSDHL	–0.71188	2.81×10^{-4}
DHCR7	–0.61551	4.44×10^{-3}
SC5D	–0.58643	1.58×10^{-6}
DHCR24	–0.52348	6.15×10^{-5}
Metabolic pathways		
MVD	–1.20200	3.25×10^{-7}
RUSC1-AS1	–1.19390	3.86×10^{-4}
FDPS	–0.99954	4.79×10^{-7}
ACLY	–0.99295	4.29×10^{-7}
LSS	–0.95937	1.97×10^{-4}
MVK	–0.89367	2.97×10^{-15}
ADC	–0.88398	1.68×10^{-4}
PCYT2	–0.82023	2.73×10^{-9}
IDI1	–0.53757	7.52×10^{-6}
GNE	–0.52270	2.09×10^{-6}
PANK3	–0.52227	1.03×10^{-7}
PGP	–0.42231	1.93×10^{-4}
Fatty acid metabolism		
ELOVL6	–1.04040	1.42×10^{-9}
FASN	–0.94224	1.06×10^{-8}
ACAT2	–0.88752	5.76×10^{-6}
SCD	–0.45186	3.13×10^{-5}
ACACA	–0.44852	9.30×10^{-6}
FADS2	–0.35183	2.15×10^{-4}

Whole gene expression analysis on NC15 treatment in JKT cells using Next Generation Sequencing. Data are expressed as the p-values which have been adjusted by using the Benjamini & Hochberg method. Corrected p-value of 0.005 was set as the threshold for significantly differential expression. TM7SF2, Transmembrane 7 superfamily member 2; MSMO1: methylsterol monooxygenase 1; HSD17B7: hydroxysteroid (17-beta) dehydrogenase 7; NSDHL: dependent steroid dehydrogenase-like; DHCR7: 7-dehydrocholesterol reductase; SC5D: sterol-C5-desaturase; DHCR24: 24-dehydrocholesterol reductase; MVD: mevalonate diphosphate decarboxylase; RUSC1-AS1: RUSC1 antisense RNA 1; FDPS: farnesyl diphosphate synthase; ACLY: ATP citrate lyase; LSS: lanosterol synthase; MVK: mevalonate kinase; ADC: arginine decarboxylase; PCYT2: phosphate cytidylyltransferase 2; IDI1: isopentenyl-diphosphate delta isomerase 1; GNE: glucosamine (UDP-N-acetyl)-2-epimerase/N-acetylmannosamine kinase; PANK3: pantothenate kinase 3; PGP: phosphoglycolate phosphatase; ELOVL6: ELOVL fatty acid elongase 6; FASN: fatty acid synthase; ACAT2: acetyl-CoA acetyltransferase 2; SCD: stearoyl-CoA desaturase; ACACA: acetyl-CoA carboxylase alpha; FADS2: fatty acid desaturase 2.

with intact membranes), and finally to Annexin V positive/ PI positive (end stage apoptosis and cell death). The presence of cells with these three phenotypes in a mixed cell population, or the transformation of a synchronized cell population through these three stages suggests apoptosis (55). However, the cells in the late apoptosis stage may not necessarily come from apoptosis, but also from necrosis and possibly other mechanism of cell death. When the plasma membrane of the cells become permeable, early apoptotic cells can become late apoptotic cells or secondary necrotic cells (56). After treatment with NC15, the late apoptotic cells might become necrotic cells, and be detected in the late apoptosis phase by the apoptosis array assay. The secondary necrotic cells were not true apoptotic cells, because the proteins associated with apoptosis such as bad, bax, BID, bcl-2, Caspase-3, Caspase-8, Cytochrome C, Fas, Fas ligand and HSP70 in the NC15-treated cells were not significantly different from those of untreated cells. To find out whether or not the cells in the late apoptotic stage were mainly derived apoptosis, we performed the apoptosis array assay and found that apoptosis might not be the main mechanism responsible for the death of JKT cells in the late apoptosis region in Figure 4. Instead, derangements in metabolic pathways may be the cause of cell death in JKT cells after NC15 treatment, because NGS data showed no changes in RNA levels and related protein expressions. Further studies are needed to elucidate the metabolic mechanism of cell death in NC15-treated JKT cells.

In conclusion, the newly derived compound NC15 can reduce cell viability and increase the percentage of cells in

the sub-G_1 phase in the JKT cells. The main mechanism of anti-cancer activity of NC15 against JKT cells may be through the up-regulation of TSG and the genes responsible for serine metabolism and aminoacyl-tRNA biosynthesis, and the down-regulation of the genes responsible for steroid biosynthesis, metabolic pathways, and fatty acid metabolism. The JKT cells may be killed by NC15 through the disturbances in their metabolism and cell cycle, rather than through apoptosis.

Conflicts of Interest

The Authors have no conflicts of interest to declare regarding this study.

Authors' Contributions

CDK designed the research, planned the research, revised and finalized the manuscript. ETT performed most of the experiments and drafted the initial manuscript. JYW synthesized the NC15 for research and improved the manuscript. FYY performed the experiment of Figure 3. JFL, HFL and YJC participated in the discussion and refined the manuscript. All Authors read and approved the manuscript.

Acknowledgements

This work was supported by the grants V104C-153 and V104E5-001 of the Taipei Veterans General Hospital, Taipei, Taiwan.

References

1 Pui CH, Gajjar AJ, Kane JR, Qaddoumi IA and Pappo AS: Challenging issues in pediatric oncology. Nat Rev Clin Oncol *8*: 540-549, 2011. PMID: 21709698. DOI: 10.1038/nrclinonc.2011.95

2 Nguyen K, Devidas M, Cheng SC, La M, Raetz EA, Carroll WL, Winick NJ, Hunger SP, Gaynon PS, Loh ML and Children's Oncology Group: Factors influencing survival after relapse from acute lymphoblastic leukemia: A Children's Oncology Group study. Leukemia *22*: 2142-2150, 2008. PMID: 18818707. DOI: 10.1038/leu.2008.251

3 Bhojwani D and Pui CH: Relapsed childhood acute lymphoblastic leukaemia. Lancet Oncol *14(6)*: e205-e217, 2013. PMID: 23639321. DOI: 10.1016/S1470-2045(12)70580-6

4 Schneider U, Schwenk HU and Bornkamm G: Characterization of EBV-genome negative "null" and "T" cell lines derived from children with acute lymphoblastic leukemia and leukemic transformed non-Hodgkin lymphoma. Intern J Cancer *19*: 621-626, 1977. PMID: 68013. DOI: 10.1002/ijc.2910190505

5 Meng XW, Heldebrant MP, Flatten KS, Loegering DA, Dai H, Schneider PA, Gomez TS, Peterson KL, Trushin SA, Hess AD, Smith BD, Karp JE, Billadeau DD and Kaufmann SH: Protein kinase Cβ modulates ligand-induced cell surface death receptor accumulation: a mechanistic basis for enzastaurin-death ligand synergy. J Biol Chem *285*: 888-902, 2010. PMID: 19887445. DOI: 10.1074/jbc.M109.057638

6 Smirnova IS, Chang S and Forsthuber TG: Prosurvival and proapoptotic functions of ERK1/2 activation in murine thymocytes *in vitro*. Cell Immunol *261*: 29-36, 2010. PMID: 19914607. DOI: 10.1016/j.cellimm.2009.10.008

7 Jin M, Park S and Pyo MY: Suppressive effects of T-412, a flavone on interleukin-4 production in T cells. Biol Pharm Bull *32*: 1875-1879, 2009. PMID: 19881301. DOI: 10.1248/bpb.32.1875

8 Wang H, Zhou CL, Lei H and Wei Q: Inhibition of calcineurin by quercetin *in vitro* and in Jurkat cells. J Biochem *147*: 185-190, 2010. PMID: 19880376. DOI: 10.1093/jb/mvp163

9 Wang GS: Medical uses of mylabris in ancient China and recent studies. J Ethnopharmacol *26*: 147-162, 1989. PMID: 2689797. DOI: 10.1016/0378-8741(89)90062-7

10 Chen YN, Chen JC, Yin SC, Wang GS, Tsauer W, Hsu SF and Hsu SL: Effector mechanisms of norcantharidin-induced mitotic arrest and apoptosis in human hepatoma cells. Intern J Cancer *100*: 158-165, 2002. PMID: 12115564. DOI: 10.1002/ijc.10479

11 Chen YJ, Shieh CJ, Tsai TH, Kuo CD, Ho LT, Liu TY and Liao HF: Inhibitory effect of norcantharidin, a derivative compound from blister beetles, on tumor invasion and metastasis in CT26 colorectal adenocarcinoma cells. Anticancer Drugs *16*: 293-299, 2005. PMID: 15711181. DOI: 10.1097/00001813-200503000-00008

12 Chen YJ, Chang WM, Liu YW, Lee CY, Jang YH, Kuo CD and Liao HF: A small molecule metastasis inhibitor, norcantharidin, downregulates matrix metalloproteinase-9 expression by inhibiting Sp1 transcriptional activity in colorectal cancer cells. Chem-Biol Interact *181*: 440-446, 2009. PMID: 19616522. DOI: 10.1016/j.cbi.2009.07.004

13 Honkanen RE: Cantharidin, another natural toxin that inhibits the activity of serine/threonine protein phosphatases types 1 and 2A. FEBS Lett 330: 283-286, 1993. PMID: 8397101. DOI: 10.1016/0014-5793(93)80889-3

14 McCluskey A, Walkom C, Bowyer MC, Ackland SP, Gardiner E and Sakoff JA: Cantharimides: a new class of modified cantharidin analogues inhibiting protein phosphatases 1 and 2A. Bioorg Med Chem Lett *11*: 2941-2946, 2001. PMID: 11677131. DOI: 10.1016/s0960-894x(01)00594-7

15 Baba Y, Hirukawa N and Sodeoka M: Optically active cantharidin analogues possessing selective inhibitory activity on Ser/Thr protein phosphatase 2B (calcineurin): implications for the binding mode. Bioorg Med Chem *13*: 5164-5170, 2005. PMID: 15951185. DOI: 10.1016/j.bmc.2005.05.013

16 Chen RT, Hua Z, Yang JL, Han JX, Zhang SY, Lü FL and Xü B: Studies on antitumor actions of cantharidin. Chin Med J *93*: 183-187, 1980. PMID: 6766849.

17 McCluskey A, Ackland SP, Bowyer MC, Baldwin ML, Garner J, Walkom CC and Sakoff JA: Cantharidin analogues: synthesis and evaluation of growth inhibition in a panel of selected tumour cell lines. Bioorg Chem *31*: 68-79, 2003. PMID: 12697169. DOI: 10.1016/s0045-2068(02)00524-2

18 Tagwireyi D, Ball DE, Loga PJ and Moyo S. Cantharidin poisoning due to 'Blister beetle' ingestion. Toxicon *38*: 1865-1869, 2000. PMID: 10858524. DOI: 10.1016/s0041-0101(00)00093-3

19 Zhang L, Sun X and Zhang ZR: An investigation on liver-targeting microemulsions of norcantharidin. Drug Deliv *12*: 289-295, 2005. PMID: 16188728. DOI: 10.1080/10717540500176829

20 Wu LT, Chung JG, Chen JC and Tsauer W: Effect of norcantharidin on *N*-acetyltransferase activity in HepG2 cells. Am J Chin Med *29*: 161-172, 2001. PMID: 11321474. DOI: 10.1142/S0192415X01000186

21 Fan YZ, Fu JY, Zhao ZM and Chen CQ: Effect of norcantharidin on proliferation and invasion of human gallbladder carcinoma GBC-SD cells. World J Gastroenterol *11*: 2431-2437, 2005. PMID: 15832413. DOI: 10.3748/wjg.v11.i16.2431

22 Li JL, Cai YC, Liu XH and Xian LJ: Norcantharidin inhibits DNA replication and induces apoptosis with the cleavage of initiation protein Cdc6 in HL-60 cells. Anticancer Drugs *17*: 307-314, 2006. PMID: 16520659. DOI: 10.1097/00001813-200603000-00009

23 Hill TA, Stewart SG, Sauer B, Gilbert J, Ackland SP, Sakoff JA and McCluskey A: Heterocyclic substituted cantharidin and norcantharidin analogues – synthesis, protein phosphatase (1 and 2A) inhibition, and anti-cancer activity. Bioorg Med Chem Lett *17*: 3392-3397, 2007. PMID: 17451951. DOI: 10.1016/j.bmcl.2007.03.093

24 Yang EB, Tang WY, Zhang K, Cheng LY and Mack PO: Norcantharidin inhibits growth of human HepG2 cell-transplanted tumor in nude mice and prolongs host survival. Cancer Lett *117*: 93-98, 1997. PMID: 9233837. DOI: 10.1016/s0304-3835(97)00206-1

25 Tsauer W, Lin JG, Lin PY, Hsu FL and Chiang HC: The effects of cantharidin analogues on xanthine oxidase. Anticancer Res 17(3C): 2095-2098, 1997. PMID: 9216670.

26 Massicot F, Dutertre-Catella H, Pham-Huy C, Liu XH, Duc HT and Warnet JM: *In vitro* assessment of renal toxicity and inflammatory events of two protein phosphatase inhibitors cantharidin and norcantharidin. Basic Clin Pharm Toxicol *96*: 26-32, 2005. PMID: 15667592. DOI: 10.1111/j.1742-7843.2005.pto960104.x

27 Chen YJ, Kuo CD, Tsai YM, Yu CC, Wang GS and Liao HF: Norcantharidin induces anoikis through Jun-*N*-terminal kinase activation in CT26 colorectal cancer cells. Anticancer Drugs *19*: 55-64, 2008. PMID: 18043130. DOI: 10.1097/CAD.0b013e3282f18826

28 Kok SH, Hong CY, Kuo MYP, Lee CHK, Lee JJ, Lou IU, Lee MS, Hsiao M and Lin SK: Comparisons of norcantharidin cytotoxic effects on oral cancer cells and normal buccal keratinocytes. Oral Oncol *39*: 19-26, 2003. PMID: 12457717. DOI: 10.1016/s1368-8375(01)00129-4

29 Wu JY, Kuo CD, Chu CY, Chen MS, Lin JH, Chen YJ and Liao HF: Synthesis of novel lipophilic *N*-substituted norcantharimide derivatives and evaluation of their anticancer activities. Molecules *19*: 6911-6928, 2014. PMID: 24865603. DOI: 10.3390/molecules19066911

30 Chang MC, Tsai ET, Wu JY, Liao HF, Chen YJ and Kuo CD: *N*-Farnesyloxy-norcantharimide and *N*-farnesyl-norcantharimide inhibit the progression of leukemia and increase survival days in a syngeneic mouse leukemia model. Anticancer Drugs *26*: 508-517, 2015. PMID: 25588161. DOI: 10.1097/CAD.0000000000000210

31 Spadavecchia S, Gonzalez-Lopez O, Carroll KD, Palmeri D and Lukac DM: Convergence of Kaposi's sarcoma-associated herpesvirus reactivation with Epstein-Barr virus latency and cellular growth mediated by the notch signaling pathway in coinfected cells. J Virol *84(20)*: 10488-10500, 2010. PMID: 20686042. DOI: 10.1128/JVI.00894-10

32 Anders S and Huber W: Differential expression analysis for sequence count data. Genome Biol *11*: R106, 2010. PMID: 20979621. DOI: 10.1186/gb-2010-11-10-r106

33 Kanehisa M, Araki M, Goto S, Hattori M, Hirakawa M, Itoh M, Katayama T, Kawashima S, Okuda S, Tokimatsu T, and Yamanishi Y: KEGG for linking genomes to life and the environment. Nucl Acids Res *36*: D480-484, 2008. PMID: 18077471. DOI: 10.1093/nar/gkm882

34 Langmead B, Trapnell C, Pop M and Salzberg SL: Ultrafast and memory-efficient alignment of short DNA sequences to the human genome. Genome Biol *10*: R25, 2009. PMID: 19261174. DOI: 10.1186/gb-2009-10-3-r25

35 Langmead B and Salzberg SL: Fast gapped-read alignment with Bowtie 2. Nat Meth *9*: 357-359, 2012. PMID: 22388286. DOI: 10.1038/nmeth.1923

36 Trapnell C, Pachter L and Salzberg SL: TopHat: discovering splice junctions with RNA-Seq. Bioinformatics *25*: 1105-1111, 2009. PMID: 19289445. DOI: 10.1093/bioinformatics/btp120

37 Don L, Huang Z, Liu D, Zhu P, Lv S, Li N and Mao H: Transcriptome analysis of chrysanthemum in responses to white rust. Sci Horticul *233*: 421-430, 2018. DOI: 10.1016/j.scienta.2018.01.016

38 Duan CX, Li DD, Sun SL, Wang XM and Zhu ZD: Rapid development of microsatellite markers for Callosobruchus chinensis using Illumina paired-end sequencing. PLoS One *9(5)*: e95458, 2014. PMID: 24835431. DOI: 10.1371/journal.pone.0095458

39 Liu J, Wang S, Qin T, Li N, Niu Y, Li D, Yuan Y, Geng H, Xiong L and Liu D: Whole transcriptome analysis of Penicillium digitatum strains treatmented with prochloraz reveals their drug-resistant mechanisms. BMC Genomics *16*: 855, 2015. PMID: 26499483. DOI: 10.1186/s12864-015-2043-x

40 Zhao HY, Song Y, Cao XN, Qin YZ, Lai YY, Jiang H, Jiang Q, Huang XJ and Kong Y: Leukemia-propagating cells demonstrate distinctive gene expression profiles compared with other cell fractions from patients with *de novo* Philadelphia chromosome-positive ALL. Ann Hematol *97(5)*: 799-811, 2018. PMID: 29429020. DOI: 10.1007/s00277-018-3253-5

41 He P, Zhang YF, Hong DY, Wang J, Wang XL, Zuo LH, Tang XF, Xu WM and He M: A reference gene set for sex pheromone biosynthesis and degradation genes from the diamondback moth, Plutella xylostella, based on genome and transcriptome digital gene expression analyses. BMC Genomics *18(1)*: 219, 2017. PMID: 28249567. DOI: 10.1186/s12864-017-3592-y

42 Liu T, Pan L, Jin Q and Cai Y: Differential gene expression analysis of benzo(a)pyrene toxicity in the clam, Ruditapes philippinarum. Ecotoxicol Environ Saf *115*: 126-136, 2015. PMID: 25686690. DOI: 10.1016/j.ecoenv.2015.02.007

43 Li Z, Liu X, Zhang P, Han R, Sun G, Jiang R, Wang Y, Liu X, Li W, Kang X, and Tian Y: Comparative transcriptome analysis of hypothalamus-regulated feed intake induced by exogenous visfatin in chicks. BMC Genomics *19(1)*: 249, 2018. PMID: 29642854. DOI: 10.1186/s12864-018-4644-7

44 Jin FJ, Han P, Zhuang M, Zhang ZM, Jin L and Koyama Y: Comparative proteomic analysis: SclR is importantly involved in carbohydrate metabolism in *Aspergillus oryzae*. Appl Microbiol Biotech *102(1)*: 319-332, 2017. PMID: 29098410. DOI: 10.1007/s00253-017-8588-7

45 Lu X, Chen X, Mu M, Wang J, Wang X, Wang D, Yin Z, Fan W, Wang S, Guo L and Ye W: Genome-wide analysis of long noncoding RNAs and their responses to drought stress in cotton (*Gossypium hirsutum* L.). PLoS One *11(6)*: e0156723, 2016. PMID: 27294517. DOI: 10.1371/journal.pone.0156723

46 Bentley DR, Balasubramanian S, Swerdlow HP, Smith GP, Milton J, Brown CG, Hall KP, Evers DJ, Barnes CL, Bignell HR, et al: Accurate whole human genome sequencing using reversible terminator chemistry. Nature *456(7218)*: 53-59, 2008. PMID: 18987734. DOI: 10.1038/nature07517

47 Reis-Filho JS: Next-generation sequencing. Breast Cancer Res *11(Suppl 3)*: S12, 2009. PMID: 20030863. DOI: 10.1186/bcr2431

48 Shendure J and Ji H: Next-generation DNA sequencing. Nat Biotechnol *26*: 1135-1145, 2008. PMID: 18846087. DOI: 10.1038/nbt1486

49 Møller MB: P27 in cell cycle control and cancer. Leuk Lymph *39(1-2)*: 19-27, 2000. PMID: 10975380. DOI: 10.3109/10428190009053535

50 Liggett WH Jr and Sidransky D: Role of the p16 tumor suppressor gene in cancer. J Clin Oncol *16*: 1197-1206, 1998. PMID: 9508208. DOI: 10.1200/JCO.1998.16.3.1197

51 Shaw PH: The role of p53 in cell cycle regulation. Pathol Res Pract *192*: 669-675, 1996. PMID: 8880867. DOI: 10.1016/S0344-0338(96)80088-4

52 Giacinti C and Giordano A: RB and cell cycle progression. Oncogene *25(38)*: 5220-5227, 2006. PMID: 16936740. DOI: 10.1038/sj.onc.1209615

53 Barger JF and Plas DR: Balancing biosynthesis and bioenergetics: metabolic programs in oncogenesis. Nat Rev Cancer *17*: R287-R304, 2010. PMID: 20699334. DOI: 10.1677/ERC-10-0106

54 Wu M, Neilson A, Swift AL, Moran R, Tamagnine J, Parslow D, Armistead S, Lemire K, Orrell J, Teich J, Chomicz S and Ferrick DA: Multiparameter metabolic analysis reveals a close link between attenuated mitochondrial bioenergetic function and enhanced glycolysis dependency in human tumor cells. Am J Physiol Cell Physiol *292*: C125-C136, 2007. PMID: 16971499. DOI: 10.1152/ajpcell.00247.2006

55 Hingorani R, Deng J, Elia J, McIntyre C and Mittar D: Detection of apoptosis using the BD Annexin V FITC assay on the BD FACSVerse™ system. BD Biosciences Aug, 2011.

56 Poon IK, Hulett MD and Parish CR: Molecular mechanisms of late apoptotic/necrotic cell clearance. Cell Death Diff *17*: 381-397, 2010. PMID: 20019744. DOI: 10.1038/cdd.2009.195

Received March 15, 2020
Revised March 24, 2020
Accepted March 26, 2020